

# Chapter 19

## Role of Transcranial Doppler Ultrasonography in Neuroanesthesia

Kazuyoshi Ishida, Atsuo Yamashita, and Mishiya Matsumoto

**Abstract** Transcranial Doppler ultrasonography (TCD) allows easy bedside monitoring of cerebral circulation and can be used repeatedly and continuously at low cost. A high level of skill is required to obtain a sonogram of an individual blood vessel through the transtemporal bone window with this technique. However, the use of transcranial color duplex imaging and the power motion mode has further facilitated the measurement of blood flow velocity in the brain by this method. Cerebral autoregulation and cerebrovascular CO<sub>2</sub> reactivity can be determined by TCD and are useful prognostic indicators in patients with cerebral infarction, subarachnoid hemorrhage, or head trauma. Transcranial Doppler ultrasonography is also suitable in evaluating cerebrovascular stenosis, vasospasm following subarachnoid hemorrhage, vascular patency following cerebral infarction and cerebral circulation in patients with intracranial hypertension. Furthermore, microemboli that have disseminated to the brain during carotid endarterectomy or cardiovascular surgery can be detected by TCD as microembolic signals. New techniques to differentiate between gaseous and solid microemboli are currently under development. We anticipate that the utility of TCD as a useful bedside monitoring tool for evaluating cerebral circulation will become increasingly recognized.

**Keywords** Transcranial Doppler ultrasonography • Cerebral autoregulation • Cerebrovascular CO<sub>2</sub> reactivity • Vasospasm • Microembolic signal

### 19.1 Introduction

Transcranial Doppler ultrasonography (TCD) was established in 1982 by Aaslid et al., who reported successful transcranial measurement of blood flow velocity in the internal carotid artery (ICA), middle cerebral artery (MCA), anterior cerebral artery (ACA), and posterior cerebral artery (PCA) using 2-MHz pulsed wave

---

K. Ishida (✉) • A. Yamashita • M. Matsumoto  
Department of Anesthesiology, Yamaguchi University Graduate School of Medicine, 1-1-1  
MinamiKogushi, Ube City, Yamaguchi 755-8505, Japan  
e-mail: [ishid002@yamaguchi-u.ac.jp](mailto:ishid002@yamaguchi-u.ac.jp)

Doppler [1]. TCD allows easy bedside monitoring of the cerebral circulation and can be used repeatedly and continuously at low cost without requiring a special dye.

In this chapter, we explain the measurement principles of and locations assessed by TCD, the parameters of physiological cerebral circulation, and the cerebrovascular responses that TCD can measure. We also provide an account of the changes that occur in cerebral blood flow velocity under various pathologic conditions, including vascular stenosis, vasospasm, and intracranial hypertension, and show how they are evaluated. In addition, we describe the characteristics of and methods for evaluating the intracranially disseminated microembolic signals that can be detected by TCD. Finally, we discuss the utility of TCD in surgical cases.

## 19.2 TCD Measurement Principles, Locations Assessed, and Procedures

Let us first look at the principles which underlie measurement in TCD. Rather than continuous ultrasonic waves, pulse waves are used to ultrasonically assess cerebral blood flow velocity. Based on the principle that ultrasonic waves are reflected by sites with substantially different acoustic impedances, TCD can isolate ultrasonic waves reflected by red blood cells circulating in a blood vessel. The frequency of these waves varies according to flow velocity (the Doppler effect), allowing the flow velocity of the circulating blood cells to be determined. Based on the known propagation velocity of ultrasonic waves in brain tissue (1,530 m/s), blood flow velocity at a given depth can be determined by measuring the propagation time of the pulsed ultrasonic waves reflected by blood cells. Ultrasonic waves at a frequency  $\leq 2$  MHz can pass through the skull, with lower frequencies penetrating deeper into the brain.

In terms of locations assessed, TCD can be used to insonate the ACA (A1), MCA (M1 and M2), PCA, and terminal portion of the ICA, as well as the anterior and posterior communicating arteries, through the temporal bone window. The ophthalmic artery can be visualized through the transorbital window, while the basilar artery and vertebral artery can be visualized through the transforaminal window. The external carotid artery can be insonated from the submandibular region (Fig. 19.1).

Doppler signals obtained by TCD can be visualized as sonograms by adjusting the depth of each target blood vessel (Fig. 19.2). From these sonograms, peak systolic velocity (PSV), end-diastolic velocity (EDV), and mean flow velocity ( $V_{\text{mean}}$ ) can be determined, and, subsequently from these values, the pulsatility index (PI) can be calculated:

$$PI = (PSV - EDV) \cdot V_{\text{mean}}^{-1} \quad (19.1)$$

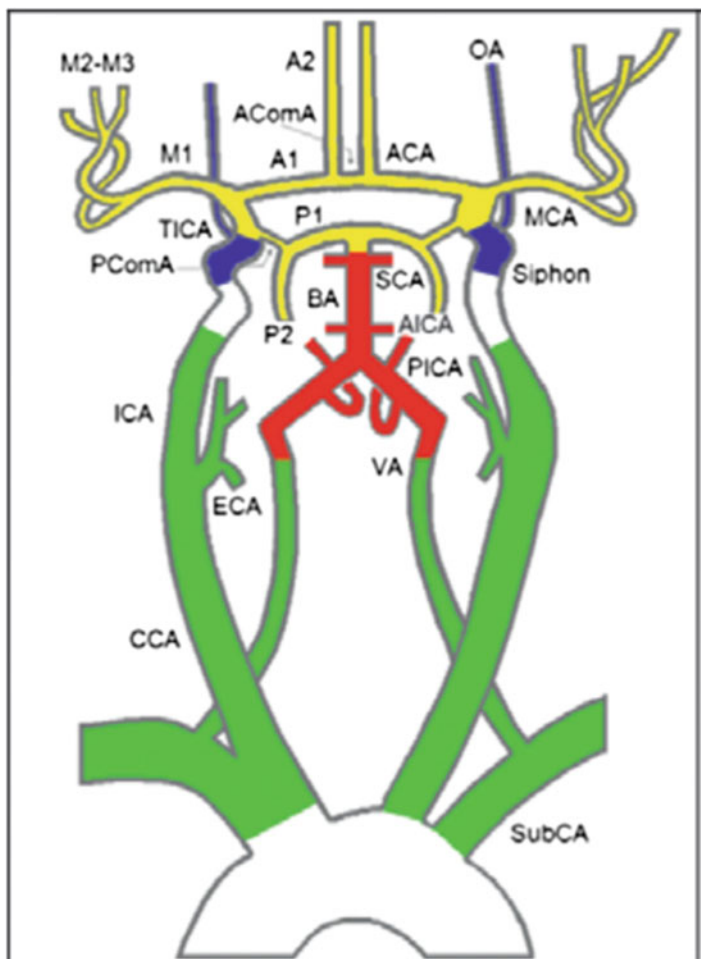


**Fig. 19.1** Insonation area of cervicocerebral vasculature by transcranial Doppler. *Yellow*, through transtemporal window; *blue*, through transorbital window; *red*, through foraminous window; and *green*, through submandibular region. *MCA* indicates middle cerebral artery, and *M1*, *M2* and *M3* are segments of this artery; *ACA* indicates anterior cerebral artery, and *A1* and *A2* are segments of this artery; *P1* and *P2* are segments of posterior cerebral artery; *CCA*, *ICA*, and *ECA* indicate common, internal, and external carotid arteries; *TICA* indicates the terminal portion of *ICA*; *siphon* indicates siphon portion of *ICA*; *SCA* indicates superior cerebellar artery; *AComA* and *PComA* indicates anterior and posterior communicating arteries; *BA* indicates basilar artery; *AICA* and *PICA* indicate anterior and posterior inferior cerebellar arteries; *OA* indicate ophthalmic artery; *VA* indicates vertebral artery; *SubCA* indicates subclavian artery. (Adapted and modified from reference [36])

Usually, the  $V_{mean}$  value in the *MCA*, where the ultrasonic irradiation angle is almost parallel to the blood flow, provides the most accurate estimate of blood flow velocity. Blood flow velocity in the *MCA* can be detected at a depth of 35–65 mm, with a  $V_{mean}$  of 45–70 cm/s. The *MCA* is the only artery whose  $V_{mean}$  can be constantly determined at a depth of  $\geq 20$  mm. However, since 10 % of patients lack

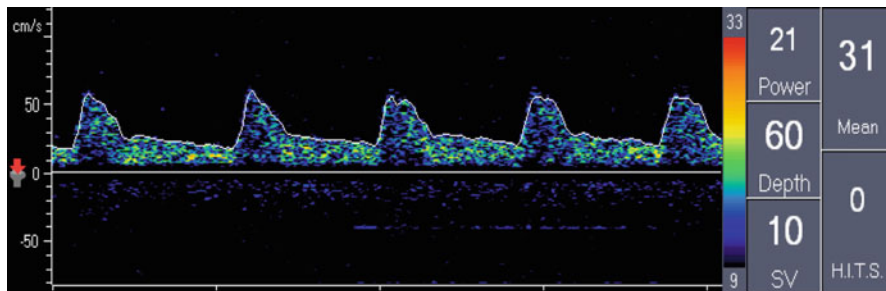


**Fig. 19.2** Typical sonogram pattern of the middle cerebral artery blood flow velocity and envelope. *Top white envelope curve* indicates estimated maximum velocity

a temporal bone window, insonation of the MCA is difficult in some cases, especially in elderly and female patients [2].

Although a high level of skill is required to obtain a sonogram of an individual blood vessel through the transtemporal bone window by TCD, recent technical innovations have facilitated the visualization of blood vessels. One such innovation is transcranial color duplex imaging, where the depth and blood flow of blood vessels are transcranially visualized by color Doppler imaging (Fig. 19.3). With this technique, the depth, location, and sample volume of the target vessel can be determined. Another innovation is the power motion mode, which enables the identification and visualization of all blood vessels in the Doppler beam by collecting blood flow information from multiple sample volumes (usually 8) within the range of the set depth (Fig. 19.4).

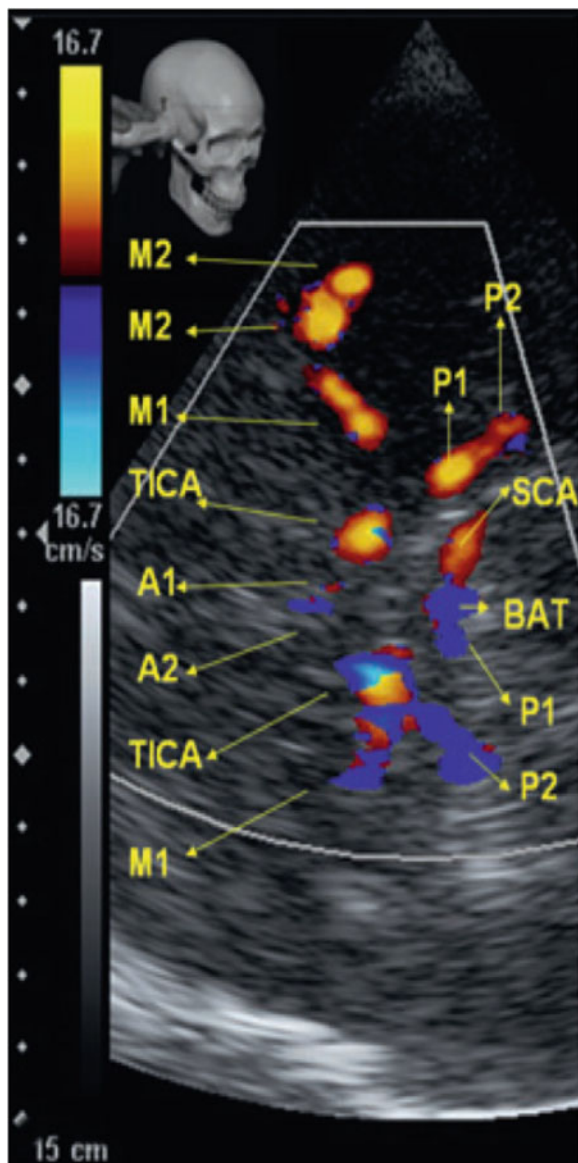
### 19.3 Physiological Parameters Measurable by TCD

TCD measures only the blood flow velocity of insonated cerebral blood vessels, not actual blood flow. Thus, assuming that the diameter of the target blood vessel is not significantly affected by physiological changes, any change in cerebral blood flow velocity should reflect a relative change in cerebral blood flow. In fact, the diameter of the MCA, as measured by magnetic resonance imaging or visually by craniotomy, does not substantially change, even with a change in blood pressure, CO<sub>2</sub> load, or stand-up load [3–5]. Furthermore, V<sub>mean</sub> as determined by TCD correlates well with cerebral blood flow velocity as measured by N<sub>2</sub>O inhalation (as described by Kety and Schmidt) or <sup>133</sup>Xe inhalation [6], suggesting that changes in V<sub>mean</sub> reflect relative changes in cerebral blood flow.

#### 19.3.1 Evaluation of Cerebral Autoregulation

Cerebral autoregulation (CA) is a mechanism that maintains the cerebral blood flow at a constant level against varying mean arterial blood pressure (MAP). There are

**Fig. 19.3** Normal vessel appearance on transtemporal transcranial color duplex imaging *M1* and *M2* indicate M1 and M2 segments of the middle cerebral artery; *TICA* indicates terminal portion of the internal carotid artery; *A1* and *A2* indicate segments of the anterior cerebral artery; *P1* and *P2* indicate segments of the posterior cerebral artery; *SCA* indicates superior cerebellar artery; *BAT* indicates basilar artery. (Adapted and modified from reference [36])



two types of CA: static CA, which maintains cerebral blood flow against a mild change in MAP, and dynamic CA, which maintains cerebral blood flow against a rapid change in MAP. Evaluating CA is important because impaired CA results in either decreased blood pressure, which is associated with an increased risk of cerebral ischemia, or increased blood pressure, which is associated with an increased risk of cerebral hemorrhage.

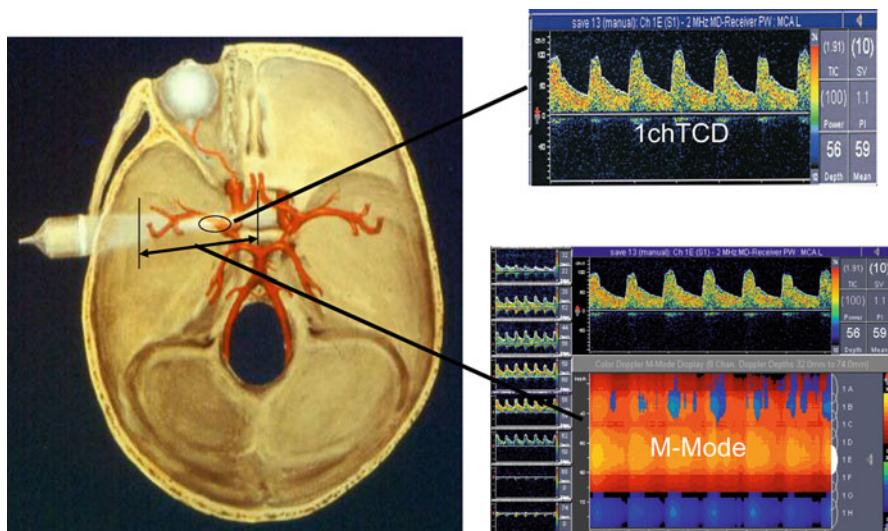


**Fig. 19.4** Power motion mode enables identification and visualization of all blood vessels in Doppler beam by collecting blood flow information from multiple sample volumes (usually eight) within range of set depth

### 19.3.1.1 Evaluation of Static CA

Slow and continuous intravenous infusion of phenylephrine in increments of 20 mmHg gradually increases MAP. Mean arterial pressure and  $V_{\text{mean}}$  are measured before and after phenylephrine infusion. The percent change in cerebral vascular resistance (%CVR) per percent change in MAP (%MAP) is calculated as static CA (sCA%) using the following formulas:

$$\text{sCA}\% = \text{\%CVR} \cdot \text{\%MAP}^{-1} \quad (19.2)$$

$$\text{CVR} = \text{MAP} \cdot V_{\text{mean}}^{-1};$$

$$\text{\%CVR} = (\text{CVR pre} - \text{CVR post}) \text{CVR pre}^{-1} \quad (19.3)$$

$$\text{\%MAP} = (\text{MAP pre} - \text{MAP post}) \cdot \text{MAP pre}^{-1} \quad (19.4)$$

Here,  $\text{sCA}\% \geq 20$  is defined as normal vascular response [7].

It is typically understood that cerebral blood flow is regulated to maintain the MAP between 60 and 150 mmHg [8]. However, recent studies using TCD have shown that  $V_{\text{mean}}$  increases slightly depending on even this range of MAP at a constant rate [9].

### 19.3.1.2 Evaluation of Dynamic CA

Even after a rapid change in MAP, dynamic CA settles the cerebral blood flow to a constant level within 5 s. Dynamic CA can be evaluated by TCD by inducing a rapid change in blood pressure by mechanical or chemical stimulation or by making use of spontaneous fluctuations in MAP.

#### Suprasystolic Thigh Cuff Method

After inflating a thigh cuff to achieve a blood pressure of 30 mmHg above the systolic level and maintaining it for 2–3 min, rapid release of the cuff decreases MAP by about 15 mmHg. As a parameter of dynamic CA against this rapid change in MAP, the rate of regulation (RoR) is calculated as follows:

$$\text{RoR} = (\Delta\text{CVR} \cdot \Delta t^{-1} \cdot \Delta\text{MAP}^{-1}) \quad (19.5)$$

The change in MAP is measured over 2.5 s, from 1 to 3.5 s after cuff release, where CVR is calculated by multiplying MAP by  $V_{\text{mean}}^{-1}$  and  $\Delta t$  is 2.5 s (Fig. 19.5a) [10].  $V_{\text{mean}}$  decreases with decrease in MAP over the first 1 s after cuff release, after which CVR decreases with continued decreases in MAP (Fig. 19.5b) and  $V_{\text{mean}}$  recovers to the level before cuff release. The normal value for RoR is 20 and a value close to 0 indicates impaired dynamic CA [10]. The autoregulation index is calculated by normalizing the pattern of change in  $V_{\text{mean}}$  over time so that evaluation can be made by determining which pattern most accurately describes the observed change in  $V_{\text{mean}}$  (Fig. 19.5c). An autoregulation index of  $\geq 5$  is defined as normal dynamic CA [10].

#### Valsalva Maneuver

The effect of the Valsalva maneuver on the systemic and cerebral circulation is manifested in four stages: stage I, in which holding of inspiration increases intrathoracic pressure, causing blood to be pumped out of the chest cavity and MAP and  $V_{\text{mean}}$  to increase; stage IIa, in which decreased venous return results in decreased cardiac output and MAP, while increased intrathoracic pressure results in increased intracranial pressure and decreased  $V_{\text{mean}}$ ; stage IIb, in which sympathicotonia results in increased cardiac output and recovery of MAP, while  $V_{\text{mean}}$  also improves as a result of improved blood pressure and dynamic CA; stage III, in which a decrease in intrathoracic pressure following expiration of intrathoracic air results in decreased MAP due to blood inflow into the chest cavity; and stage IV, in which improved venous return leads to an increase in MAP and  $V_{\text{mean}}$  (Fig. 19.6). To evaluate dynamic CA, the autoregulatory slope index (ASI) is calculated by



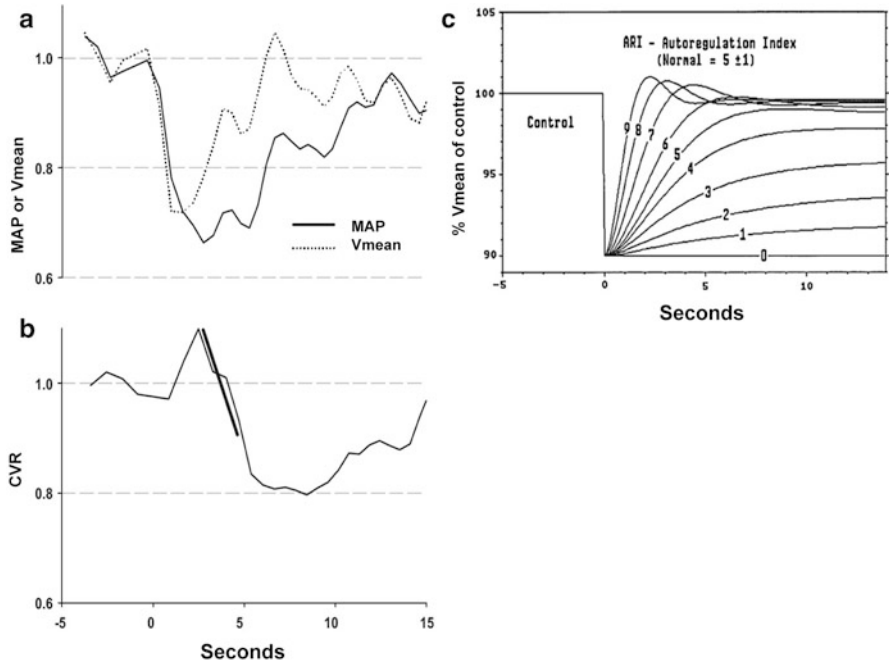


**Fig. 19.5** Typical changes in mean arterial pressure (MAP), mean flow velocity (Vmean) (a), and cerebrovascular resistance in response to suprasystolic thigh cuff deflation to determine dynamic cerebral autoregulation (b). MAP and Vmean decreased simultaneously during first second after tight cuff was released following earlier recovery of Vmean during next seconds than MAP (a). All tracings are shown in normalized units relative to control prerelease values from -4 to 0 s. Straight line (bold line) through cerebral vascular resistance curve (b) was determined by regression analysis of data obtained from 1 to 3.5 s after thigh cuff release and used to calculate rate of regulation. Autoregulation index was calculated by normalizing pattern of change in Vmean over time so that evaluation could be made by determining which pattern most accurately described observed change in Vmean (c) (Adapted and modified from reference [10])

incorporating the duration of stage IIa and the degree of improvement in MAP and Vmean into the following formula:

$$ASI = \left\{ \left[ (Vmean_{(IIa+3s)} - Vmean_{(IIa)}) \cdot Vmean_{(IIa)}^{-1} - (MAP_{(IIa+3s)} - MAP_{(IIa)}) \cdot MAP_{(IIa)}^{-1} \right] \times 100 \right\} \quad (19.6)$$

The normal range of ASI in healthy individuals has been reported to be  $22 \pm 14 \%$  [11].

### Postural Alterations

Standing up from a supine, sitting, or squatting position can cause MAP to change by up to 35 mmHg. Dynamic CA can be evaluated based on changes in MAP and Vmean determined by this *postural alterations* method.



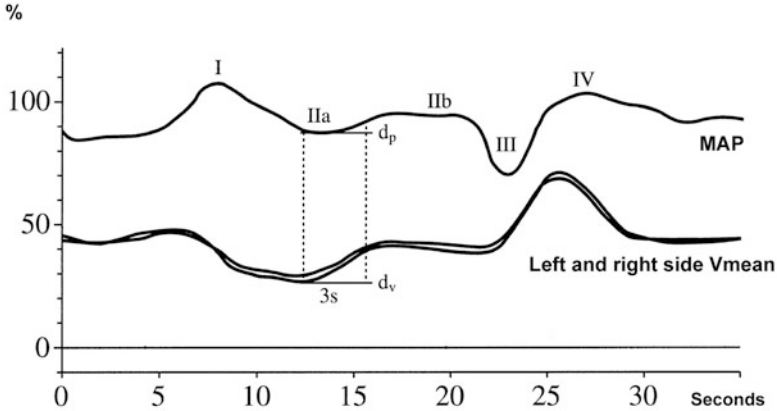


**Fig. 19.6** Recordings of MAP and Vmean during Valsalva maneuver. Phase I, increased intrathoracic and MAP; phase IIa, fall in arterial blood pressure due to decreased atrial filling; phase IIb, rise in MAP due to increased heart rate; phase III, sudden decrease in MAP due to release of intrathoracic pressure; and phase IV, overshoot in MAP with resumed atrial filling. Derivation of autoregulatory slope index is shown:  $d_v$ , difference between minimum Vmean and Vmean reading 3 s later, and  $d_p$ , difference between MAP readings in the same time interval (Adapted and modified from reference [11])

### Transient Hyperemic Response Ratio

The transient hyperemic response ratio (THRR) is calculated by dividing the mean PSV from the average of two heart beats after the release of 5-s common carotid artery compression (PSV hyperemia), as measured by ipsilateral TCD, by the mean PSV from the average of five heart beats before compression (PSV baseline), as follows:

$$\text{THRR} = (\text{PSV hyperemia} \cdot \text{PSV baseline}^{-1}) \quad (19.7)$$

With normal dynamic CA, cerebral blood vessels on the compressed side will be dilated to increase blood flow during carotid artery compression, resulting in transient hyperemia after releasing compression. The normal range for THRR is  $1.2 \pm 0.04$ , and a value close to 1 indicates impaired dynamic CA [12].

### Spontaneous Fluctuations in Blood Pressure

Blood pressure fluctuates finely, even at rest. CA has been evaluated by examining the correlation between low-frequency MAP fluctuation ( $\leq 2.0$  Hz) and Vmean. The correlation coefficient between the average values of Vmean and MAP over 5–10 s is calculated as the mean velocity index (Fig. 19.7a). Impaired dynamic CA is associated with a higher positive correlation between Vmean and MAP

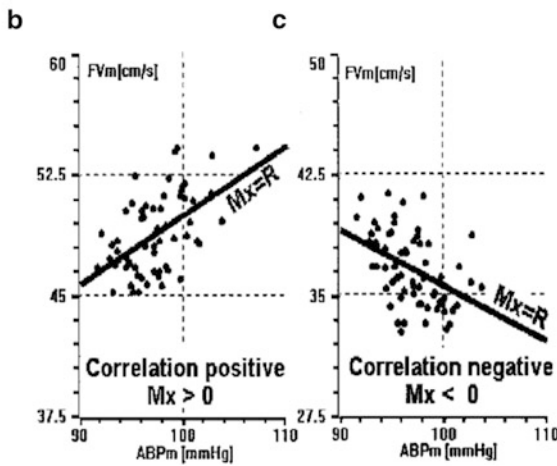
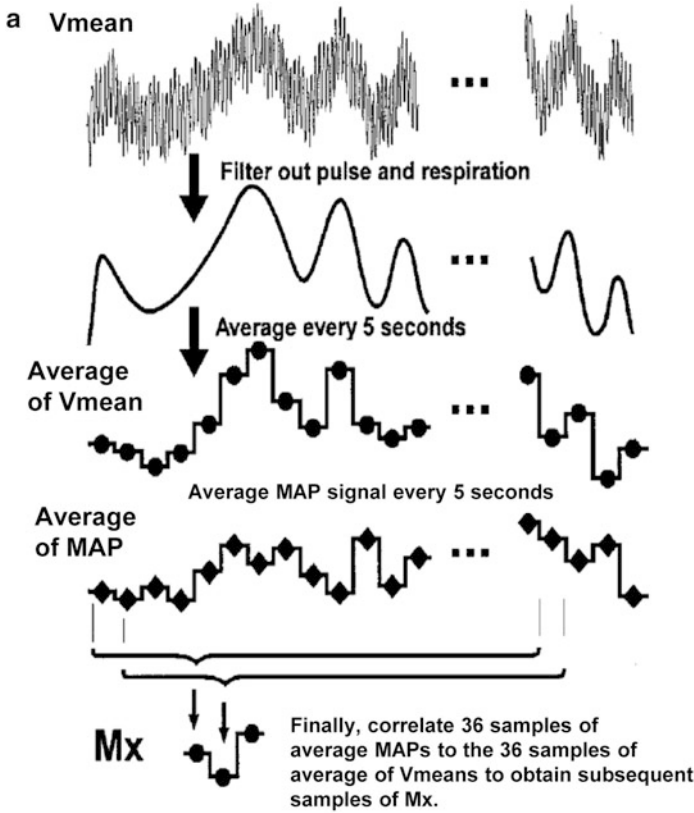


**Fig. 19.7** Signal processing steps used to obtain subsequent samples of mean velocity index (Mx) (a). Two examples of linear regression plots with positive and negative values of Mx corresponding to non-autoregulating (b) and autoregulating (c) systems, respectively (Adapted and modified from reference [13])

(Fig. 19.7b), while normal dynamic CA is associated with no or a negative correlation (Fig. 19.7c) [13].

### 19.3.1.3 Effect of Anesthetics on CA

When evaluating CA by TCD during surgery, consideration should be given to the type of anesthetic being used. Volatile inhalation anesthetics typically used in clinical practice such as desflurane, sevoflurane, and isoflurane are known to impair CA in a dose-dependent manner. In contrast, intravenous anesthetic propofol reduces  $V_{\text{mean}}$ , but does not affect CA. Opioids such as fentanyl and remifentanyl do not affect  $V_{\text{mean}}$  or CA [14].

### 19.3.1.4 Significance of Evaluating CA

Evaluation of CA by TCD has been performed under various pathologic conditions. Impaired CA is observed in the presence of cerebral vascular spasms in patients with post-subarachnoid hemorrhage [15]. Cerebral infarction, even involving small lesions, is also associated with impaired CA. The degree of impaired CA initially worsens over the first 5 days after the onset of cerebral infarction, but gradually improves over the 3 months that follow. There is also a correlation between the degree of impaired CA after cerebral infarction and the severity and prognosis of brain disorder [16]. Furthermore, CA evaluation has proven prognostic utility in patients with head trauma [17–19].

## 19.3.2 Evaluation of Cerebrovascular $\text{CO}_2$ Reactivity

Cerebrovascular  $\text{CO}_2$  reactivity ( $\text{CO}_2$  R) can be evaluated by challenge with chemicals such as acetazolamide or by changing the arterial partial pressure of  $\text{CO}_2$  ( $\text{PaCO}_2$ ) through respiratory regulation. Acetazolamide increases the tissue concentration of  $\text{CO}_2$  by inhibiting carbonic anhydrase, an enzyme catalyzing the conversion of  $\text{CO}_2$  and water to bicarbonate, thereby inducing metabolic acidosis in tissue.

$\text{PaCO}_2$  can be changed by rebreathing of  $\text{CO}_2$ , administering  $\text{CO}_2$ , or changing the respiratory rate consciously to hypoventilation, apnea, and hyperventilation.  $\text{CO}_2$  R is calculated as follows:

$$\text{Absolute } \text{CO}_2\text{R} = \Delta V_{\text{mean}} \cdot \Delta \text{PaCO}_2^{-1} \quad (19.8)$$

$$\begin{aligned} & \text{Relative CO}_2\text{R (percentage of baseline Vmean)} \\ &= (\text{absolute CO}_2\text{R} \cdot \text{baseline Vmean}^{-1}) \cdot 100 \end{aligned} \quad (19.9)$$

Here,  $\Delta$  represents the change in each parameter before and after changing PaCO<sub>2</sub>.

### 19.3.2.1 Effect of Anesthetics on CO<sub>2</sub> R

When evaluating CO<sub>2</sub> R by TCD during surgery, consideration should be given to the effect of anesthetics on CO<sub>2</sub> R, as in the case of evaluating CA. Volatile inhalation anesthetics such as desflurane, sevoflurane, and isoflurane are known to increase CO<sub>2</sub> R by increasing Vmean. In contrast, CO<sub>2</sub> R can be maintained with the intravenous anesthetic propofol, although the CO<sub>2</sub> R value will be slightly lower due to a reduced baseline Vmean. Opioids do not affect CO<sub>2</sub> R [20].

### 19.3.2.2 Significance of Evaluating CO<sub>2</sub> R

CO<sub>2</sub> R is decreased in patients with hypertension [21], obstructive apnea syndrome [22], central apnea syndrome complicated by heart failure [23], or carotid artery stenosis [24]. In addition, a correlation exists between an increased blood cholesterol level, a known precipitating factor for arteriosclerosis, and reduced CO<sub>2</sub> R in patients with a history of mild cerebral infarction or transient ischemic attack [25]. In patients with carotid artery stenosis and reduced CO<sub>2</sub> R, an increased incidence of cerebral infarction has been observed during follow-up [26–28]. Furthermore, impaired CO<sub>2</sub> R has been shown to correlate with the prognosis in patients with head trauma complicated by cerebral hemorrhage [29].

In patients with kidney disorder, however, controversy remains as to whether CO<sub>2</sub> R is maintained [30] or impaired [31]. Similarly in diabetic patients, some studies have reported an increased CO<sub>2</sub> R during general anesthesia [32], while others have reported a decreased CO<sub>2</sub> R [33]. Given that decreased CO<sub>2</sub> R during anesthesia is likely associated with postoperative cognitive dysfunction [34], evaluating CO<sub>2</sub> R is also important in predicting the risk of brain disorder and patient outcome.

## 19.4 Pathologic Conditions Evaluable by TCD

### 19.4.1 Intracranial Vascular Stenosis

Intracranial vascular stenosis can be detected by TCD as a localized area with an increase in PSV and Vmean. It has been reported that  $\geq 50\%$  stenosis in the MCA

corresponds to a  $V_{\text{mean}}$  of 80–100 cm/s and 70 % stenosis corresponds to a  $V_{\text{mean}}$  of 110–120 cm/s [35]. A change in blood flow velocity in the distal part of the narrowing vessel can be detected as a decrease in  $V_{\text{mean}}$  to <30 cm/s and a decrease in PI to <0.6 (vasodilatation). A decreased  $V_{\text{mean}}$  and an increased PI are evident at the proximal part of the stenosis (Fig. 19.8). In the presence of severe stenosis in the ICA, the blood flow in the ipsilateral ACA is reversed, flowing from the contralateral side to the stenotic side through the circle of Willis.

### ***19.4.2 Vasospasm***

Vasospasm caused by subarachnoid hemorrhage can be easily detected and evaluated by TCD and occurs along a longer length of blood vessels than intracranial stenotic lesions. Vasospasm in the MCA can be most accurately detected by TCD as an area with increased  $V_{\text{mean}}$  and PSV. The criteria for identifying vasospasm are shown in Table 19.1. Since vasospasm is present even before a patient develops clinical symptoms or cerebral infarction, evaluating  $V_{\text{mean}}$  by TCD in post-subarachnoid hemorrhage patients is important in the early detection and treatment planning of vasospasm [36].

### ***19.4.3 Acute Ischemic Stroke, Occlusion, Recanalization, and Reperfusion***

TCD is useful in evaluating cerebrovascular patency in patients with cerebral infarction. The thrombolysis in brain ischemia [37] and consensus on grading intracranial flow obstruction criteria [38] are used to evaluate blood flow (Fig. 19.9), and cerebrovascular patency based on these criteria is considered to correlate strongly with patient outcome.

### ***19.4.4 Evaluation of Intracranial Pressure***

TCD can be used to evaluate cerebral perfusion pressure and also to indirectly evaluate intracranial pressure (ICP). The initial sign of increased ICP is a combination of decreased EDV and increased PI. End-diastolic velocity becomes zero after ICP has exceeded diastolic blood pressure and decreases to negative values, with further increases in ICP (reverse diastolic flow), resulting in decreased PSV and eventually blood flow undetectable on TCD (Fig. 19.10). The sensitivity and specificity of undetectable blood flow on TCD for brain death are 95 % and 100 %, respectively.

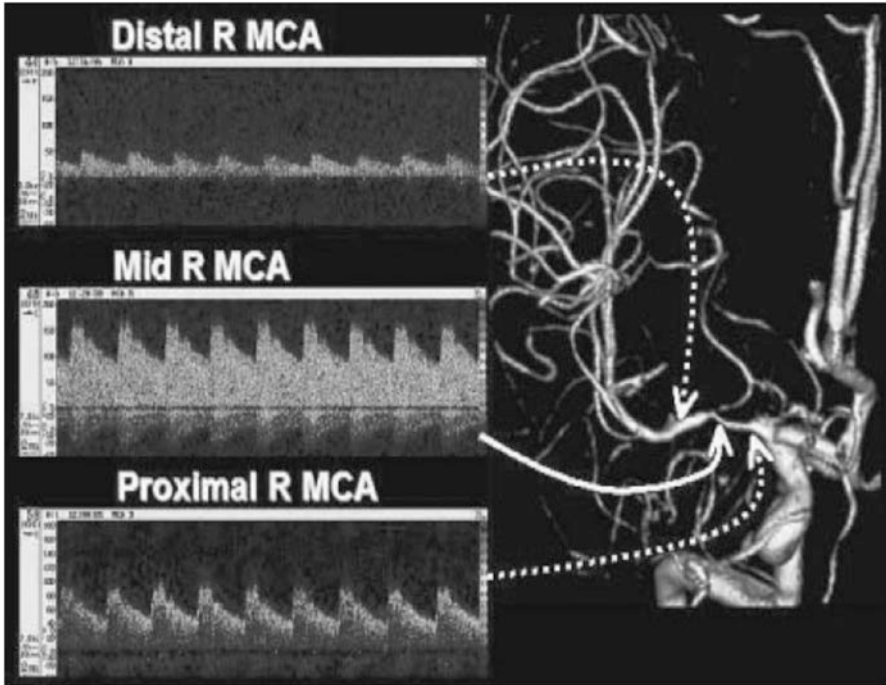


**Fig. 19.8** Spectrogram changes in right middle cerebral artery with stenosis are displayed on corresponding magnetic resonance angiograph. Significant increase in flow velocities in stenotic region (peak systolic velocity 120 cm/s) and decrease in post-stenotic region are evident (Adapted and modified from *Neurosonology* 19:113–131, 2006, in Japanese; URL: [https://www.jstage.jst.go.jp/article/neurosonology/19/3/19\\_3\\_113/\\_pdf](https://www.jstage.jst.go.jp/article/neurosonology/19/3/19_3_113/_pdf))

**Table 19.1** Criteria for identifying vasospasm

MCA (M1 and M2) vasospasm	Vmean (cm/s)	PSV (cm/s)	MCA/ECICA ratio
Severe	>200	>300	>6.0
Moderate	150–200	250–300	4.5–5.9
Mild	120–150	200–250	3.0–4.5

MCA middle cerebral artery, Vmean mean flow velocity, PSV peak systolic velocity, ECICA extracranial internal carotid artery

### 19.5 Detection of Microembolic Signals

The concept of microembolic signals (MES) was first introduced in 1965 by Austen et al., who detected signals that were stronger and shorter than those of blood flow sound in a cardiopulmonary bypass circuit using continuous ultrasonic waves [39]. Because they used a bubble-type oxygenation device for the cardiopulmonary bypass circuit, they assumed that these MES represented gaseous microemboli. In

Category	Appearance	Description
TIBI 0 COGIF 1		<b>ABSENT FLOW</b> No flow signal
TIBI 1 COGIF 2		<b>MINIMAL FLOW</b> Systolic spikes with variable velocity and duration; zero EDV; reverberating flow
TIBI 2 COGIF 3		<b>BLUNTED FLOW</b> Systolic upstroke delayed (duration >0.20 sec); EDV>0; PI<1.2
TIBI 3 COGIF 3		<b>DAMPENED FLOW</b> Vmean decrease greater than 30% of contralateral value; upstroke normal; EDV>0
TIBI 4 COGIF 4c		<b>HYPEREMIC FLOW</b> Segmentally increased flow velocities (Vmean >80 cm/s and/or >30% compared to the control side, no turbulence; low PI; no harmonics; low degree spectral broadening.
TIBI 4 COGIF 4b		<b>PSEUDOSTENOTIC FLOW</b> Focally increased flow velocities ( Vmean >30% compared to the control side; EDV>0; Significant turbulence or flow disturbance.
TIBI 5 COGIF 4a		<b>NORMAL FLOW</b> Flow velocities normal or in the range of $\pm 30\%$ of the control side. [* Bar: 50 cm/sec]

**Fig. 19.9** Thrombolysis in brain ischemia (TIBI) and consensus on grading intracranial flow obstruction (COGIF) criteria: patients with absent flow (TIBI grade 0, COGIF grade 1), minimal flow with zero EDV (TIBI grade 1, COGIF grade 2), and low flow with either blunted (TIBI grade 2) or dampened (TIBI grade 3, COGIF grade 3) configuration show worse prognosis than patients with flow velocities equal to those of contralateral side (TIBI grade 5, COGIF grade 4a), flow velocities that increased segmentally (TIBI grade 4, COGIF grade 4c), or flow velocities that increased focally (COGIF grade 4b) (Adapted and modified from reference [36])

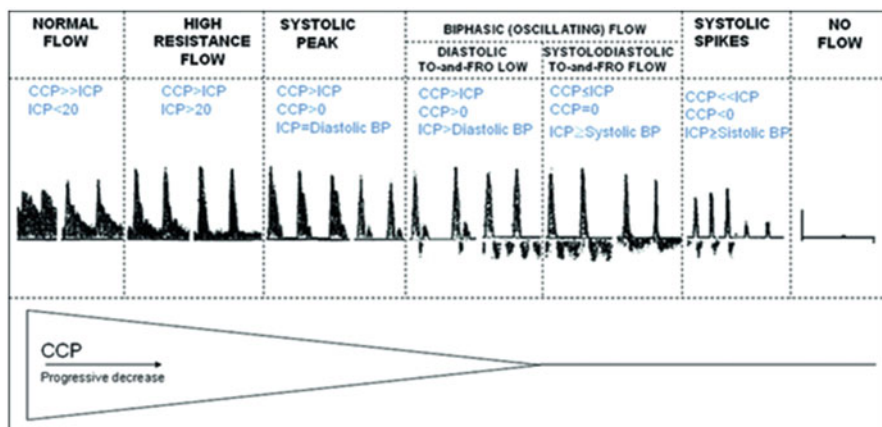


**Fig. 19.10** Increased progressive waveform changes with intracranial pressure (ICP), eventually leading to cerebral circulatory arrest. If ICP significantly to level obviating spontaneous cerebral circulation (i.e., cerebral circulatory arrest or brain death), transcranial Doppler will show one of following specific flow patterns: (1) alternating flow with systolic forward flow, followed by complete reversal during diastole, indicating net zero forward flow, or (2) systolic peaks with only systolic hit to stagnant blood column but no flow: CPP, cerebral perfusion pressure. (Adapted and modified from reference [36])



1986, MES were detected during TCD-monitored carotid endarterectomy (CEA) [40]. This was the first study to detect intraoperatively disseminated microemboli in the brain by TCD. However, since this was observed after cutting the ICA, it was again considered that these MES represented gaseous microemboli. Subsequently, in 1990, MES with different acoustic properties than those of gaseous microemboli were detected during CEA. Because they were detected before cutting the ICA, these MES were considered to originate from solid microemboli such as a thrombus or atheroma. Patients in whom solid microemboli-derived MES were detected developed transient ischemic attack or cerebral infarction after surgery [41]. Subsequently, TCD was also applied in cardiovascular surgery to measure and detect MES.

### ***19.5.1 Definition of MES***

MES are defined as signals with a characteristic sound on a TCD sonogram. They are characterized by a signal intensity of  $\geq 3$  dB stronger than the background blood flow sound and a duration of  $< 300$  msec [42, 43] (Fig. 19.11). To detect MES, gain and ultrasonic power should be set as low as possible so that the background flow spectrum is barely visible.

### ***19.5.2 Differentiation Between Gaseous and Solid MES***

A number of attempts have been made since around 2002 to differentiate between gaseous and solid MES [44]. Because gaseous microemboli have very low acoustic impedance, Doppler signals are strongly reflected at the interface. Thus, MES representing gaseous microemboli are observed as strong signals on TCD [41]. However, it is difficult to differentiate relatively small gaseous microemboli from solid microemboli.

Microembolic signals comprise sine waves at a constant frequency (Fig. 19.11). It is believed that gaseous and solid MES can be differentiated to some extent by analyzing their frequencies, as gaseous MES emit relatively high-frequency sound ( $> 400$ – $500$  Hz) (Fig. 19.11a, b), while solid MES emit sound at a lower frequency ( $\leq 400$  Hz) (Fig. 19.11c, d) [45]. Russel et al. differentiated the two types of MES by using ultrasonic waves of two different frequencies (2 MHz and 2.5 MHz) based on the fact that gaseous MES reflect 2-MHz ultrasonic waves more strongly than 2.5-MHz ones (Fig. 19.12a), while solid MES reflect ultrasonic waves of both frequencies to a similar extent (Fig. 19.12b) [44].

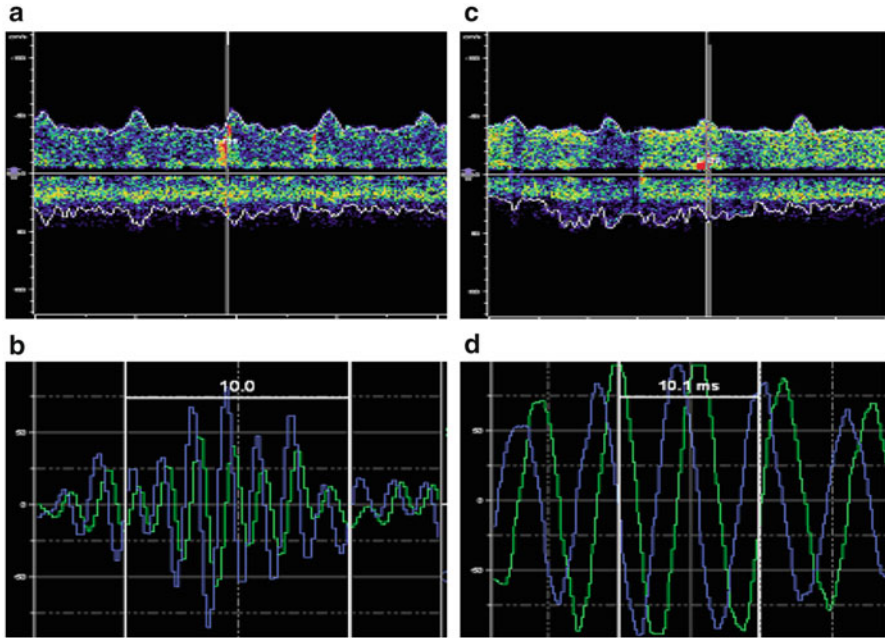


**Fig. 19.11** Microembolic signals (MES) comprise sine waves of constant frequency. Gaseous and solid MES can be differentiated to some extent by analyzing their frequencies. For MES detected on sonogram in (a), MES comprising seven sine waves were detected over 10 ms (b). Therefore, their frequency was calculated as 700 Hz, indicating gaseous MES. For MES detected on sonogram in (c), MES comprising  $\leq 2$  sine waves were detected over 10 ms (d). Therefore, their frequency was calculated as  $\leq 200$  Hz, indicating solid MES [45]

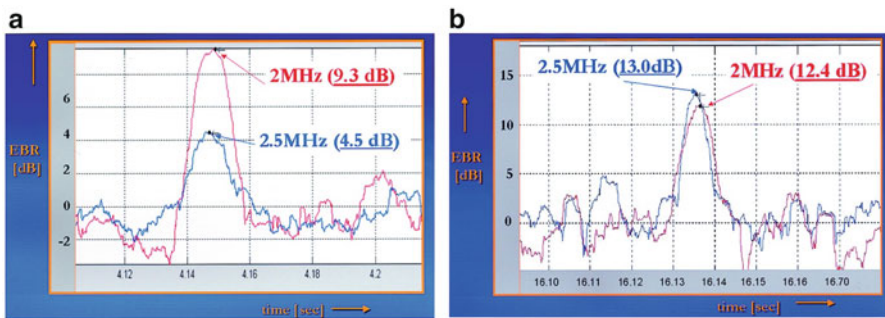


**Fig. 19.12** Gas bubble reflecting 4.8-dB greater ultrasound at 2.0-MHz insonation (red) than at 2.5 MHz (blue) (a). Solid microemboli (80- $\mu$ m plastic microsphere) reflecting only 0.6-dB greater ultrasound at 2.5-MHz insonation (blue) than at 2.0-MHz insonation (red) (b) (Adapted and modified from reference [44])

## 19.6 Usefulness of Intraoperative Monitoring by TCD

Transcranial Doppler ultrasonography is a useful monitoring tool that allows for the bedside monitoring of various parameters. However, it has limited use intraoperatively during neurosurgical procedures. Its utility has therefore been demonstrated mainly in CEA and cardiovascular surgery.

### 19.6.1 Usefulness of TCD in CEA

It is helpful to monitor  $V_{\text{mean}}$  in the MCA on the operated side during CEA. During CEA, an extreme decrease in  $V_{\text{mean}}$  from the baseline indicates the need to maintain blood pressure with drugs or use a shunt tube. A study investigating the relationship between  $V_{\text{mean}}$  of the MCA during carotid occlusion during CEA under local anesthesia and the occurrence of neurological complications suggested that a  $V_{\text{mean}}$  of  $<25$  cm/s or a decrease to  $<48$  % of the baseline value represents a risk of neurological complications [46]. A decrease in  $V_{\text{mean}}$  to  $<10$  % of the baseline value during carotid occlusion and an increase in PI to  $>100$  % after clamp release are associated with cerebral infarction in the perioperative period [47]. Furthermore, the detection of  $>50$  MES during CEA is associated with cerebral ischemia [48].

Taken together, the evidence level of TCD in CEA is classes II to III, with a recommendation level of type B [49].

### 19.6.2 Usefulness of TCD in Coronary Artery Bypass Grafting Surgery

MES have been reported to occur during cardiovascular surgery in a number of cases, and their association with cerebral disorder or postoperative cognitive dysfunction has been examined. In coronary artery bypass grafting surgery (CABG) using cardiopulmonary bypass MES have been frequently detected during aortic cannulation, release of aortic cross-clamping, and heart displacement to identify the anastomotic site [50]. Furthermore, MES are even more frequently detected during valvular surgery involving cardiotomy [51].

The relationship between MES and postoperative cognitive dysfunction was confirmed in only 5 of 15 reports (1994–2009) that examined this relationship primarily in CABG cases [52]. Thus, the evidence level of MES detection by TCD during cardiovascular surgery is classes II to III, with a recommendation level of type B, while the recommendation level for the clinical significance of MES detection is type U [49].

One possible reason for the ambiguous relationship between MES detection and postoperative cognitive dysfunction after cardiovascular surgery is the small

sample size. Moreover, there have been no studies on the differential effect of gaseous and solid MES—which affect the brain differently—on the occurrence of postoperative cognitive dysfunction [52]. Fat globules aspirated from the surgical field during cardiovascular surgery can be disseminated to the brain via cardiopulmonary bypass [53]. Early and robust formation of cerebral edema in a rat model of fat emboli to the brain indicates the seriousness of such lipid dissemination [54]. It is, however, unclear whether fat emboli are detectable as MES. Further efforts to detect and differentiate MES to the maximum extent possible and prevent the dissemination of microemboli to the brain may improve the usefulness of TCD during cardiovascular surgery.

## 19.7 Conclusion

Inexpensive and noninvasive Vmean monitoring by TCD, which can provide various types of information at the bedside, is extremely useful in perioperative patient management. The use of transcranial color duplex imaging and power motion mode has further facilitated the determination of Vmean. New techniques for differentiating MES are also under development. We anticipate that the utility of TCD as a useful bedside monitoring tool will be increasingly recognized.

## References

1. Aaslid R, Markwalder TM, Nornes H (1982) Noninvasive transcranial Doppler ultrasound recording of flow velocity in basal cerebral arteries. *J Neurosurg* 57(6):769–774
2. Itoh T, Matsumoto M, Handa N et al (1993) Rate of successful recording of blood flow signals in the middle cerebral artery using transcranial Doppler sonography. *Stroke* 24(8):1192–1195
3. Giller CA, Bowman G, Dyer H et al (1993) Cerebral arterial diameters during changes in blood pressure and carbon dioxide during craniotomy. *Neurosurgery* 32(5):737–742
4. Valdueza JM, Balzer JO, Villringer A et al (1997) Changes in blood flow velocity and diameter of the middle cerebral artery during hyperventilation: assessment with MR and transcranial Doppler sonography. *AJNR Am J Neuroradiol* 18(10):1929–1934
5. Serrador JM, Picot PA, Rutt BK et al (2000) MRI measures of middle cerebral artery diameter in conscious humans during simulated orthostasis. *Stroke* 31(7):1672–1678
6. Wintermark M, Sesay M, Barbier E et al (2005) Comparative overview of brain perfusion imaging techniques. *Stroke* 36(9):e83–e99
7. Tiecks FP, Lam AM, Aaslid R et al (1995) Comparison of static and dynamic cerebral autoregulation measurements. *Stroke* 26(6):1014–1019
8. Paulson OB, Strandgaard S, Edvinsson L (1990) Cerebral autoregulation. *Cerebrovasc Brain Metab Rev* 2(2):161–192
9. Lucas SJ, Tzeng YC, Galvin SD et al (2010) Influence of changes in blood pressure on cerebral perfusion and oxygenation. *Hypertension* 55(3):698–705
10. Willie CK, Colino FL, Bailey DM et al (2011) Utility of transcranial Doppler ultrasound for the integrative assessment of cerebrovascular function. *J Neurosci Methods* 196(2):221–237

11. Tiecks FP, Douville C, Byrd S et al (1996) Evaluation of impaired cerebral autoregulation by the Valsalva maneuver. *Stroke* 27(7):1177–1182
12. Smielewski P, Czosnyka M, Kirkpatrick P et al (1996) Assessment of cerebral autoregulation using carotid artery compression. *Stroke* 27(12):2197–2203
13. Piechnik SK, Yang X, Czosnyka M et al (1999) The continuous assessment of cerebrovascular reactivity: a validation of the method in healthy volunteers. *Anesth Analg* 89(4):944–949
14. Dagal A, Lam AM (2009) Cerebral autoregulation and anesthesia. *Curr Opin Anaesthesiol* 22(5):547–552
15. Soehle M, Czosnyka M, Pickard JD et al (2004) Continuous assessment of cerebral autoregulation in subarachnoid hemorrhage. *Anesth Analg* 98(4):1133–1139
16. Aries MJ, Elting JW, De Keyser J et al (2010) Cerebral autoregulation in stroke: a review of transcranial Doppler studies. *Stroke* 41(11):2697–2704
17. Czosnyka M, Smielewski P, Kirkpatrick P et al (1996) Monitoring of cerebral autoregulation in head-injured patients. *Stroke* 27(10):1829–1834
18. Czosnyka M, Smielewski P, Lavinio A et al (2008) An assessment of dynamic autoregulation from spontaneous fluctuations of cerebral blood flow velocity: a comparison of two models, index of autoregulation and mean flow index. *Anesth Analg* 106(1):234–239
19. Lam JM, Hsiang JN, Poon WS (1997) Monitoring of autoregulation using laser Doppler flowmetry in patients with head injury. *J Neurosurg* 86(3):438–445
20. Brian JE Jr (1998) Carbon dioxide and the cerebral circulation. *Anesthesiology* 88(5):1365–1386
21. Serrador JM, Sorond FA, Vyas M et al (2005) Cerebral pressure-flow relations in hypertensive elderly humans: transfer gain in different frequency domains. *J Appl Physiol* 98(1):151–159
22. Reichmuth KJ, Dopp JM, Barczy SR et al (2009) Impaired vascular regulation in patients with obstructive sleep apnea: effects of continuous positive airway pressure treatment. *Am J Respir Crit Care Med* 180(11):1143–1150
23. Xie A, Skatrud JB, Khayat R et al (2005) Cerebrovascular response to carbon dioxide in patients with congestive heart failure. *Am J Respir Crit Care Med* 172(3):371–378
24. Widder B, Kleiser B, Krapf H (1994) Course of cerebrovascular reactivity in patients with carotid artery occlusions. *Stroke* 25(10):1963–1967
25. Wijnhoud AD, Koudstaal PJ, Dippel DW (2006) Relationships of transcranial blood flow Doppler parameters with major vascular risk factors: TCD study in patients with a recent TIA or nondisabling ischemic stroke. *J Clin Ultrasound* 34(2):70–76
26. Silvestrini M, Vernieri F, Pasqualetti P et al (2000) Impaired cerebral vasoreactivity and risk of stroke in patients with asymptomatic carotid artery stenosis. *JAMA* 283(16):2122–2127
27. Markus H, Cullinane M (2001) Severely impaired cerebrovascular reactivity predicts stroke and TIA risk in patients with carotid artery stenosis and occlusion. *Brain* 124(3):457–467
28. Vernieri F, Pasqualetti P, Matteis M et al (2001) Effect of collateral blood flow and cerebral vasomotor reactivity on the outcome of carotid artery occlusion. *Stroke* 32(7):1552–1558
29. Klingelhofer J, Sander D (1992) Doppler CO<sub>2</sub> test as an indicator of cerebral vasoreactivity and prognosis in severe intracranial hemorrhages. *Stroke* 23(7):962–966
30. Skinner H, Mackaness C, Bedford N et al (2005) Cerebral haemodynamics in patients with chronic renal failure: effects of haemodialysis. *Br J Anaesth* 94(2):203–205
31. Ishida K, Uchida M, Utada K et al (2011) Cerebrovascular carbon dioxide reactivity during general anesthesia in the patients with chronic renal failure. *J Neurosurg Anesthesiol* 23(4):459
32. Kawata R, Nakakimura K, Matsumoto M et al (1998) Cerebrovascular CO<sub>2</sub> reactivity during anesthesia in patients with diabetes mellitus and peripheral vascular disease. *Anesthesiology* 89(4):887–893
33. Kadoi Y, Hinohara H, Kunimoto F et al (2003) Diabetic patients have an impaired cerebral vasodilatory response to hypercapnia under propofol anesthesia. *Stroke* 34(10):2399–2403
34. Kadoi Y, Kawauchi C, Kuroda M et al (2011) Association between cerebrovascular carbon dioxide reactivity and postoperative short-term and long-term cognitive dysfunction in patients with diabetes mellitus. *J Anesth* 25(5):641–647

35. Feldmann E, Wilterdink JL, Kosinski A et al (2007) The Stroke Outcomes and Neuroimaging of Intracranial Atherosclerosis (SONIA) trial. *Neurology* 68(24):2099–2106
36. Topcuoglu MA (2012) Transcranial Doppler ultrasound in neurovascular diseases: diagnostic and therapeutic aspects. *J Neurochem* 123(Suppl 2):39–51
37. Demchuk AM, Burgin WS, Christou I et al (2001) Thrombolysis in brain ischemia (TIBI) transcranial Doppler flow grades predict clinical severity, early recovery, and mortality in patients treated with intravenous tissue plasminogen activator. *Stroke* 32(1):89–93
38. Nedelmann M, Stolz E, Gerriets T et al (2009) Consensus recommendations for transcranial color-coded duplex sonography for the assessment of intracranial arteries in clinical trials on acute stroke. *Stroke* 40(10):3238–3244
39. Austen WG, Howry DH (1965) Ultrasound as a method to detect bubbles or particulate matter in the arterial line during cardiopulmonary bypass. *J Surg Res* 5:283–284
40. Padayachee TS, Gosling RG, Bishop CC et al (1986) Monitoring middle cerebral artery blood velocity during carotid endarterectomy. *Br J Surg* 73(2):98–100
41. Spencer MP, Thomas GI, Nicholls SC et al (1990) Detection of middle cerebral artery emboli during carotid endarterectomy using transcranial Doppler ultrasonography. *Stroke* 21(3):415–423
42. Stroke (1995) Basic identification criteria of Doppler microembolic signals. Consensus Committee of the Ninth International Cerebral Hemodynamic Symposium. *Stroke* 26(6):1123
43. Ringelstein EB, Droste DW, Babikian VL et al (1998) Consensus on microembolus detection by TCD. International Consensus Group on Microembolus Detection. *Stroke* 29(3):725–729
44. Russell D, Brucher R (2002) Online automatic discrimination between solid and gaseous cerebral microemboli with the first multi-frequency transcranial Doppler. *Stroke* 33(8):1975–1980
45. Hanzawa K, Furui E, Ohzeki H et al (1998) Frequency analysis of high intensity transient signals in CPB can distinguish solid embolic signals from gaseous signals. *Ann Thorac Surg* 66:1490
46. Moritz S, Kasprzak P, Arlt M et al (2007) Accuracy of cerebral monitoring in detecting cerebral ischemia during carotid endarterectomy: a comparison of transcranial Doppler sonography, near-infrared spectroscopy, stump pressure, and somatosensory evoked potentials. *Anesthesiology* 107(4):563–569
47. Ackerstaff RG, Moons KG, van de Vlasakker CJ et al (2000) Association of intraoperative transcranial doppler monitoring variables with stroke from carotid endarterectomy. *Stroke* 31(8):1817–1823
48. Levi CR, O'Malley HM, Fell G et al (1997) Transcranial Doppler detected cerebral microembolism following carotid endarterectomy. High microembolic signal loads predict postoperative cerebral ischaemia. *Brain* 120(4):621–629
49. Sloan MA, Alexandrov AV, Tegeler CH et al (2004) Assessment: transcranial Doppler ultrasonography: report of the Therapeutics and Technology Assessment Subcommittee of the American Academy of Neurology. *Neurology* 62(9):1468–1481
50. Clark RE, Brillman J, Davis DA et al (1995) Microemboli during coronary artery bypass grafting. Genesis and effect on outcome. *J Thorac Cardiovasc Surg* 109(2):249–258
51. Braekken SK, Reinvang I, Russell D et al (1998) Association between intraoperative cerebral microembolic signals and postoperative neuropsychological deficit: comparison between patients with cardiac valve replacement and patients with coronary artery bypass grafting. *J Neurol Neurosurg Psychiatry* 65(4):573–576
52. Kruijs RW, Vlasveld FA, Van Dijk D (2010) The (un)importance of cerebral microemboli. *Semin Cardiothorac Vasc Anesth* 14(2):111–118
53. Brooker RF, Brown WR, Moody DM et al (1998) Cardiomy suction: a major source of brain lipid emboli during cardiopulmonary bypass. *Ann Thorac Surg* 65(6):1651–1655
54. Gohara T, Ishida K, Nakakimura K et al (2010) Temporal profiles of aquaporin 4 expression and astrocyte response in the process of brain damage in fat embolism model in rats. *J Anesth* 24(2):225–233